water

MDPI

Article

Nested Recharge Systems in Mountain Block Hydrology: High-Elevation Snowpack Generates Low-Elevation Overwinter Baseflow in a Rocky Mountain River

Éowyn M. S. Campbell * and M. Cathryn Ryan

Geosciences Department, University of Calgary, Calgary, AB T2N 1N4, Canada; cryan@ucalgary.ca
* Correspondence: eowyn.campbell@ucalgary.ca

Abstract: The majority of each year's overwinter baseflow (i.e., winter streamflow) in a third-order eastern slopes tributary is generated from annual melting of high-elevation snowpack which is transmitted through carbonate and siliciclastic aquifers. The Little Elbow River and its tributaries drain a bedrock system formed by repeated thrust faults that express as the same siliciclastic and carbonate aquifers in repeating outcrops. Longitudinal sampling over an 18 km reach was conducted at the beginning of the overwinter baseflow season to assess streamflow provenance. Baseflow contributions from each of the two primary aquifer types were apportioned using sulfate, $\delta^{34}S_{SO4}$, and silica concentrations, while $\delta^{18}O_{H2O}$ composition was used to evaluate relative temperature and/or elevation of the original precipitation. Baseflow in the upper reaches of the Little Elbow was generated from lower-elevation and/or warmer precipitation primarily stored in siliciclastic units. Counterintuitively, baseflow generated in the lower-elevation reaches originated from higher-elevation and/or colder precipitation stored in carbonate units. These findings illustrate the role of nested flow systems in mountain block recharge: higher-elevation snowmelt infiltrates through fracture systems in the cliff-forming—often higher-elevation—carbonates, moving to the lower-elevation valley through intermediate flow systems, while winter baseflow in local flow systems in the siliciclastic valleys reflects more influence from warmer precipitation. The relatively fast climatic warming of higher elevations may alter snowmelt timing, leaving winter water supply vulnerable to climatic change.

Keywords: mountain aquifer recharge; mountain block hydrology; baseflow; isotope geochemistry; $\delta^{34}S_{SO4}$; $\delta^{18}O_{H2O}$

Citation: Campbell, É.M.S.; Ryan, M.C. Nested Recharge Systems in Mountain Block Hydrology: High-Elevation Snowpack Generates Low-Elevation Overwinter Baseflow in a Rocky Mountain River. *Water* **2021**, *13*, 2249. https://doi.org/10.3390/w13162249

Academic Editor: Manuela Lasagna

Received: 14 July 2021
Accepted: 12 August 2021
Published: 18 August 2021

Highlights

- Nested flow systems convey higher-elevation/colder precipitation to lower-elevation river reaches;
- Winter baseflow is generated mainly from winter precipitation stored and transported through carbonate aquifers;
- Long flow pathways for high-elevation precipitation suggest little difference between intermediate and deep flow pathways and therefore between mountain aquifer and mountain block recharge;
- Dependence on winter precipitation leaves the river vulnerable to climate change.

1. Introduction

Mountain streamflow provides water to more than 1 billion people worldwide, with increasing demand expected in coming decades [1]. Mountain catchments often receive much of their precipitation as snow [2] and are warming faster than lowlands [3], leaving them vulnerable to observed changes in snowfall and snowmelt [4]. Understanding how streamflow is generated is crucial to understanding how to manage climate change in these

watersheds, particularly in the parts of the hydrologic year with the lowest streamflow (i.e., the baseflow season).

Mountain block hydrology refers to recharge and streamflow generation processes in areas of high topographic relief [5]. The term mountain block recharge (MBR) denotes water delivered from the mountain block to lowland aquifers by deep or regional flow systems rather than the processes of recharge within the mountain block itself [5,6], which Markovich et al. [6] suggest can be referred to as "mountain aquifer recharge". This distinction may be necessary because of the historical usage of the term MBR, but it is debatable whether there is any real differentiation in the processes of recharging local, intermediate, and regional flow systems within a mountain block. In mountain headwaters, precipitation can be stored and released as streamflow from coarse deposits such as talus slopes, rock glaciers, and moraines [7,8] as well as alluvial aquifers [9]. Though orders of magnitude less permeable, bedrock infiltration in these environments is also significant due to lack of soil in alpine regions, high topographic relief [10] and fracturing. Manning et al. [11] indicate that approximately 10% of infiltrated water moves into deep or regional flow pathways, and along with previous modelling studies, suggest the majority of bedrock infiltration remains in the uppermost ~20 m with higher permeability, resurfacing as mountain streamflow [6,7,12]. Somers and McKenzie [2] list numerous studies identifying groundwater contributions to mountain streamflow was greater than 50% in many cases. These findings correspond to the results of previous hydrologic modelling in the Elbow River watershed, where the provenance of up to 60% of spring and summer streamflow in the Elbow River was bedrock aquifers, and the remaining "interflow" contribution had relatively short residence times in coarse, shallow groundwater systems before becoming streamflow [12]. Thus, recharge processes in mountain block hydrology deserve closer focus.

While groundwater contribution to mountain streamflow, is well established [2,13,14] a robust understanding of the seasonal variability and intricacies of streamflow generation in a given watershed is required when managing land-use and climate change. A good example is the part of the hydrologic year with the lowest streamflow. In the Rocky Mountains in western North America, this period is overwinter baseflow, important where mountain and lowland populations alike rely year round on mountain streamflow. In cold regions where winter precipitation falls as snow and does not contribute to streamflow in that same season, winter baseflow is necessarily groundwater generated. However, which groundwater? Do all possible aquifers in the watershed contribute? How old is the winter baseflow water—did it fall as last year's rain and snow, or that from a century ago?

Manning et al. [11] demonstrated that low vertical permeability produces distinct stratification in mountain groundwaters, with the majority of younger circulation occurring in the upper 20 m. Paznekas and Hayashi [15] showed that the winter baseflow rate in several Rocky Mountain watersheds is not dependent on the volume of precipitation from the previous year, suggesting a "fill and spill" model for the aquifers, and Campbell et al. [12] demonstrated that in an eastern slopes Rocky Mountain river, up to 20% of winter baseflow is derived from the previous winter's snowmelt, implying relatively rapid cycling through the hydrogeologic system. Similarly, Campbell et al. [16] found an average groundwater residence time of ~4 years for streamflow. Somers and McKenzie [2] highlight the 'buffering capacity' that groundwater storage provides for streamflow in dry seasons and drought and suggest that it may provide some resilience to climate change. With mountain aquifer residence times of only a few years in some systems, this capacity may be limited.

To better understand the resilience of a given watershed, it is ideal to understand where precipitation infiltrates, in which hydrogeologic units it is stored during groundwater transport, and becomes streamflow, and the time scales of each. Water isotopes in precipitation and streamflow have long been used as intrinsic tracers to estimate mean travel times for water through watersheds [17,18] (see for example [19]) and also provide information about the relative temperature and/or elevation of the original precipitation (i.e., warmer, lower-elevation vs. colder, higher-elevation) i.e., [20–22]. Dissolved ions within streamflow can provide information about the type(s) of rock–water interaction,

and hence the aquifer(s) where the water was stored after infiltration and before discharge into rivers as groundwater baseflow. Dissolved silica has been used with water oxygen isotopes to evaluate transit times [23–25] and can also provide insight about rock–water interaction and therefore host aquifers [26–28]. Campbell et al. [16] used silica and sulfate, along with sulfur isotopes in sulfate, to define a three-end-member mixing model that differentiated spring and summer aquifer contributions to the Elbow River. This method can be further applied to assess source-aquifer contributions to overwinter baseflow, and these findings used to assess resilience of the Elbow River watershed to climatic change.

Although aquifer types and average streamflow age have been evaluated for eastern slopes of the Rocky Mountain rivers, such as the Elbow River, there is no work on determining the relative contributions of different aquifer transport pathways and recharge elevations during the critical seasonal period where streamflow is dominantly groundwater baseflow. To evaluate these pathways for early winter baseflow, we conducted longitudinal streamflow sampling along a reach of the Elbow River (akin to a seepage run [28] but for sampling as opposed to discharge measurements) at the end of the open water season. Thirteen samples were collected over an 18 km reach, stretching from the mouth of the groundwater/surface water transition (i.e., headwater) of the Little Elbow to above its confluence with the Big Elbow, and collated the results from open water season streamflow sampling (July). All samples were analyzed for silica and sulfate concentrations and water and sulfate isotope compositions. We demonstrate that winter baseflow in the Little Elbow is mainly generated from high-elevation winter precipitation which is primarily stored in carbonate aquifers. High-elevation regions are particularly susceptible to climate change [4], which leaves winter streamflow vulnerable to changes in melt patterns and reduced snowfall.

Objectives:

1. Assess relative contributions of aquifer types to baseflow;
2. Assess relative temperature and elevation of precipitation contributing to baseflow along the length of the river;
3. Use these assessments to integrate conceptualization of local, intermediate, and deep flow pathways in mountain aquifer and mountain block recharge.

2. Materials and Methods

2.1. Study Area

The Little Elbow River is one of two mainstem rivers that join to form the Elbow River, an eastern slopes Rockies river. Most of the Elbow River's flow is generated in the 435 km^2 Upper Elbow River watershed (defined here as the reach of the Elbow River upstream of Elbow Falls, Figure 1; [29,30]). Open water season is typically April to October, with peak flow in mid-May to late June due to snowmelt and seasonal rainfall. Overwinter precipitation (November–April) falls as snow and therefore does not contribute to streamflow in those months, thus overwinter streamflow (described hereafter as overwinter baseflow) is groundwater sourced. Despite the relatively long course of the Big Elbow (relative to the Little Elbow) tributary, the Big Elbow was observed to be ephemeral, with water levels dropping to more than 2 m below ground surface in the stream bed by mid-September in 2016–2018 (data not shown). Thus, between October and May, streamflow in the Elbow River is principally supplied by the Little Elbow. This supply is important as the main end-use of the Elbow River municipal water supply for ~400,000 people in the City of Calgary in Alberta, Canada, as well as several smaller communities and rural uses. Elbow River streamflow is highly variable (<5 to ~50 m^3/s, and up to 1800 m^3/s in major floods [31]), which necessitated construction of the Glenmore Dam and Reservoir in 1933 for steady overwinter water supply to the city.

The upper watershed is zoned as a multi-use recreation area and has had minimal development. Although recreation remains the primary use, usage is rapidly increasing, with a 35% increase in recreational visitors between 2019 and 2021, from ~4 million to 5.4 million. At the same time, development has continued along the Elbow River and

its alluvial aquifer corridor, and development pressure in both the upper watershed and downstream is projected to increase in coming decades [32–35]. At the same time, climate change projections for the region indicate intensifying wet and dry periods, with earlier snowmelt and earlier glacial discharge [36–38].

The temperate humid climate of the Upper Elbow Watershed results from 1981–2010 average annual precipitation (1981–2010, not corrected for snow under-catch) of 665, 639, and 568 mm at three stations in and around the watershed: Elbow RS, Kananaskis, and Pocaterra stations, respectively [38]. Approximately half this annual precipitation is snow [12], with accumulation beginning November and peaking in late March. The spring melt usually begins in May and is complete in late June. Seasonally high rainfall, often coincident with snowmelt, produces peak streamflows in June [32,37].

With an average topographic slope of 25°, the mountainous Upper Elbow watershed has a maximum elevation of 3200 m above sea level (asl) and minimum 1600 m asl. A series of thrust faults repeatedly superimpose Paleozoic-age dolomite and limestone units (carbonates) over Mesozoic-age sandstone and shale units (siliciclastics), creating alternating carbonate cliffs and siliciclastic valleys [39] (Figures 1 and 2). Vegetation follows a clear elevation gradient with three major ecoregions; forested montane (5%), transitional sub-alpine (56%), and treeless alpine ecoregions (39%) [32,39]. Valley floors may have deep deposits (>12 m) of unconsolidated sediment and soil, while these deposits are less than a few meters or absent elsewhere.

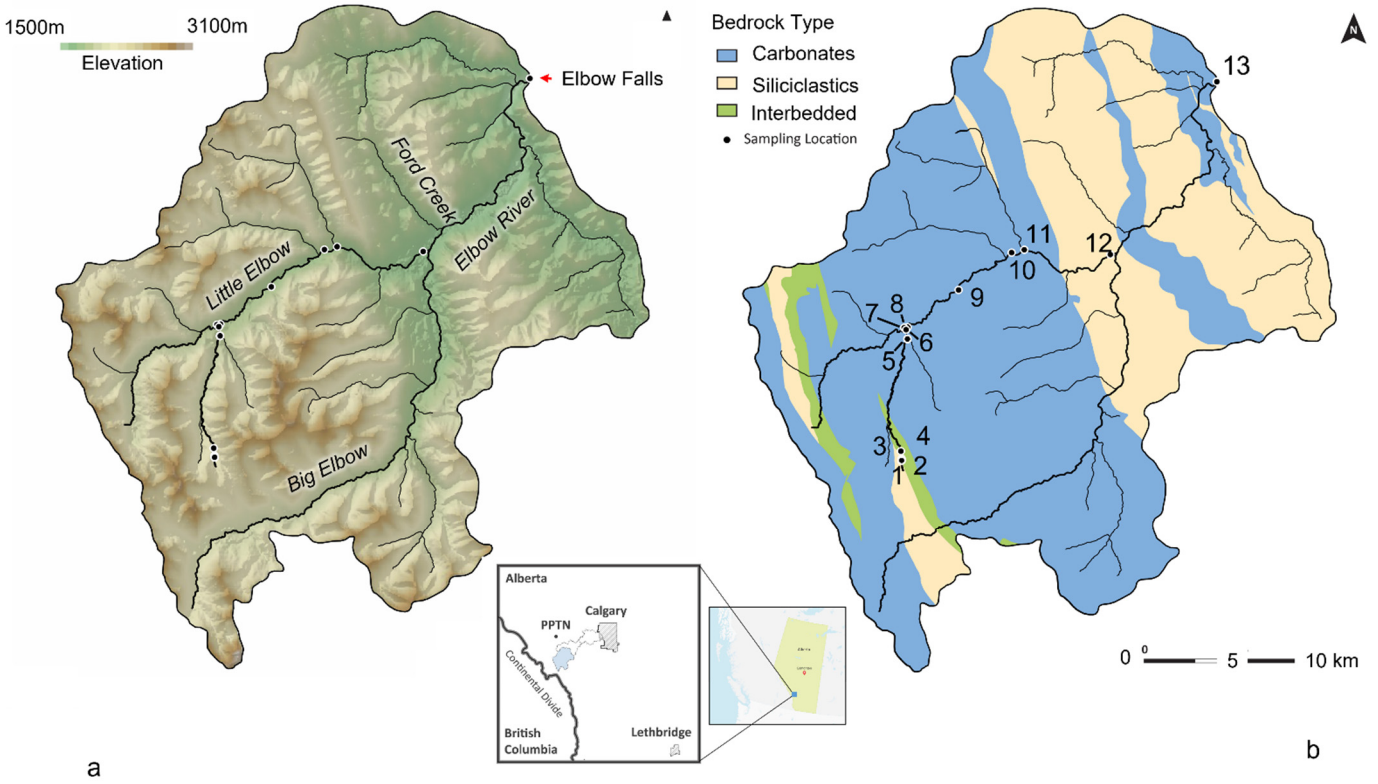

Figure 1. Upper Elbow watershed. (**a**) Linear relief shading. Sample collection points are indicated with black circles. (**b**) Watershed bedrock types. Most of the Upper Elbow watershed (including the Little Elbow where sampling was conducted) is carbonate rock (~73%), with siliciclastics upper extremities (~27%) and small areas of carbonate and siliciclastic interbedded layering. Inset shows upper (blue), middle and lower Elbow watersheds in relation to Calgary, Alberta [40]. Numbers indicate sampling locations (named in Table 1).

Table 1. Ion and Isotope Data for 26 October Longitudinal Streamflow and Representative Summer Samples.

Sampling Point Name	Point	Elevation m	Distance km	TDS mg/L	$\delta^{18}O_{H2O}$‰	$\delta^{2}H_{H2O}$‰	$\delta^{34}S_{SO4}$‰	$\delta^{18}O_{SO4}$‰	Sulfate mg/L	SiO2 mg/L	Q (Measured) m^3/s	Q (Interpolated) m^3/s	Interflow%	Siliciclastic%	Carbonate%
Little Elbow Valley First Surface Water	1	2152	0	226	−19.4	−147	−5.95	−10.65	14.3	6.94	-	0.00	13	86	2
Little Elbow Valley Headwaters	2	2150	0.05	229	−19.4	−146	−5.06	−9.07	12.7	5.35	-	0.01	33	65	2
Little Elbow Valley Main Creek	3	2148	0.1	249	−19.3	−146	−9.07	−13.33	20.9	5.85	-	0.01	24	69	7
Little Elbow Valley Bridge	4	2142	0.88	257	−19.4	−145	−6.46	−10.63	23.1	5.27	0.00	0.01	31	60	9
Base Little Elbow Valley	5	1809	6.05	300	−19.6	−147	9.64	1.49	90.2	3.92	-	0.08	28	18	54
Mt Romulus Campground	6	1797	6.7	295	−19.6	−148	0.51	−6.49	78.9	3.52	0.20	0.20	36	17	47
Piper Paradise Fisher Creek	7	1795	6.8	300	−19.5	−147	11.10	1.56	90.4	3.87	-	0.22	28	18	54
Little Elbow (First)	8	1784	6.8	296	−19.5	−147	3.46	−4.15	81.9	3.94	0.19	0.19	30	22	48
Little Elbow Mt Remus	9	1724	9.96	349	−19.7	−149	17.81	5.40	125.6	3.88	-	0.92	18	6	77
Little Elbow Bridge	10	1705	13.04	331	−19.8	−151	20.18	6.80	121.9	3.68	-	1.36	21	4	74
Nahahi Creek Above Mouth	11	1679	13.59	238	−19.1	−144	−0.66	−8.49	29.8	14.59	-	N/A			
Little Elbow (Last)	12	1605	18.37	318	−19.8	−149	18.13	5.92	105.8	3.68	-	2.14	26	10	64
Elbow Falls	13	1485	30.48	313	−19.6	−148	16.67	4.56	87.6	4.04	4.00	4.00	27	21	52
Data from Campbell et al. 2021															
Little Elbow Last (Summer)	12	1605	18.37	260	−19.7	−150	10.99	0.03	55.2	3.43	13.4		41	29	30
Elbow Falls (Summer)	13	1485	30.48	253	−19.4	−149	13.00	0.69	52.3	3.82	13.5		40	30	30

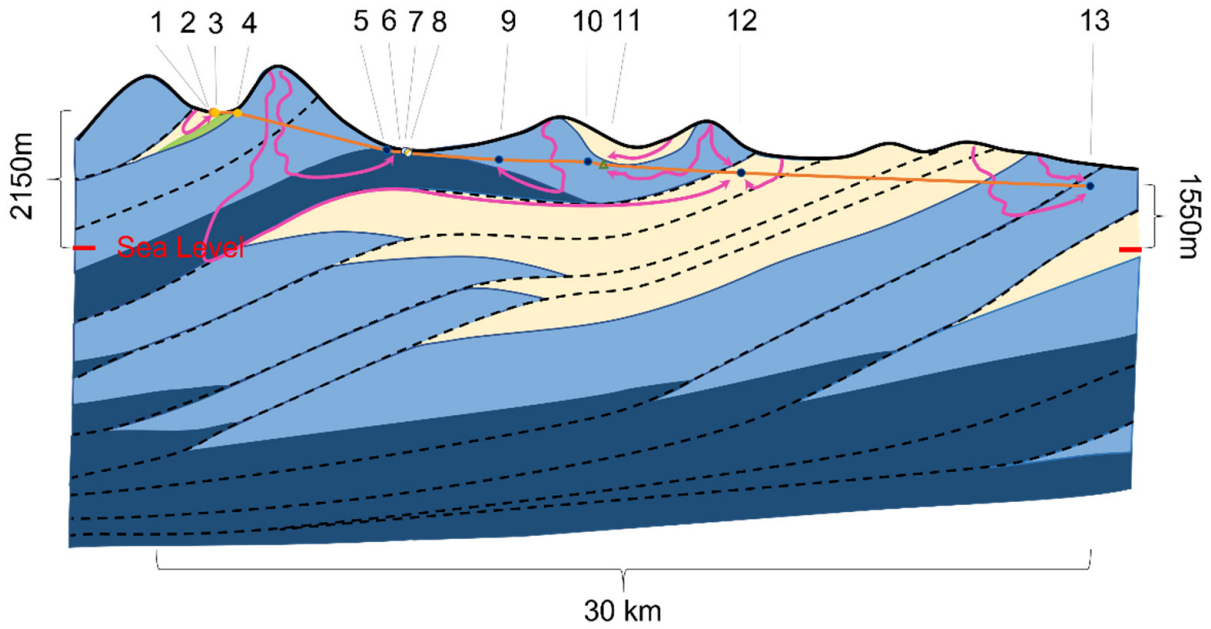

Figure 2. Schematic cross-section of the Upper Elbow Watershed (A-A′ on Figure 1) with Little Elbow River elevation profile projected (orange line). Numbers indicate the approximate location of sampling locations (yellow and blue dots (named in Table 1). Yellow units are the youngest (Mesozoic) siliciclastic rocks, green unit is Mezozoic interbedded siliciclastic and carbonate, medium blue units are younger (Upper Paleozoic) carbonates, dark blue are older (Lower Paleozoic) carbonates. Dashed lines indicate thrust faults and pink arrows illustrate some of the many possible conceptual local and intermediate flow pathways. Note the figure has significant vertical exaggeration. (Adapted from CSPG Field Guide [41]).

Figures 1 and 2 emphasize the alternating siliciclastic and carbonate rock units through which the Little Elbow flows. Krouse and Mayer [42] demonstrated that paired $\delta^{34}S_{SO4}$ and $\delta^{18}O_{SO4}$ isotopes can be used to distinguish whether SO_4 was dissolved from siliciclastic or carbonate rock, and Campbell et al. [16] used this characteristic, along with dissolved silica and sulfate concentrations, to confirm distinct water types in a three end-member mixing model for the Elbow River. The same approach, based on silica and sulphate concentrations, and dissolved sulphate isotopes are used in the present study to analyze aquifer contributions to streamflow.

Water isotopes in streamflow are used in this study to evaluate the relative elevation and temperature of precipitation before infiltration. Seasonal variability in the $\delta^{18}O$ in precipitation is considerable at high latitudes (>40‰) and varies with elevation [43,44] such that lower $\delta^{18}O$ indicates colder and/or higher-elevation precipitation. While seasonal variability is strongly dampened and lagged in streamflow in the Elbow River [12] (~2‰ intra-annually), relative variations in $\delta^{18}O_{H2O}$ in spatially separated streamflow samples collected along a river reach under steady baseflow conditions) can still provide evidence of different precipitation and infiltration regimes for source aquifers.

2.2. Sample Collection and Analysis

2.2.1. Stream Profile and Sample Points

Elbow Falls (Figure 2) is the outlet for the Upper Elbow Watershed where the river mainstem flows over bedrock falls stripped bare of alluvial gravels, which provides an integrated snapshot of the combined surface and alluvial groundwater in the watershed. Samples were collected at the mouth of the Little Elbow (sampling point 12; Figure 1) is 12 km upstream of the falls and ~100 m upstream of the seasonal confluence with the Big Elbow, adjacent to a seasonally accessible public access point. On the 26 October sampling date, surface flow in the Big Elbow had not been observed for more than two months (in

weekly sampling visits), and hence the flow at Elbow Falls was mainly from the Little Elbow tributary. The sample collection points above Little Elbow's mouth (sampling point 12) were chosen based on river accessibility with a view to longitudinal distribution along the 18 km reach that was sampled. Vehicle access above Little Elbow is normally restricted to fire suppression, but single-day access along a fire-service road was granted to facilitate the longitudinal sampling program. The first sample (transition from groundwater to surface water; sampling point 1) was the first occurrence of surface water below the remnant of Tombstone glacier in the Little Elbow Valley, and was accessed by hiking approximately 1 km from the end of the fire-service road.

The late-season October date was chosen as the latest part of the open water season (i.e., beginning of the overwinter baseflow season) with minimal likelihood of river ice formation. Sampling was conducted after seven days with no recorded precipitation. The relatively short days in late-October imposed additional time constrictions on field work, but twelve samples were collected over the 18 km length reach. At each sampling point, location and elevation were recorded with a handheld GPS. The flow distance was estimated by detailed tracing in Google Earth Pro.

Sampling point 1 is the groundwater/surface water transition in the uppermost headwaters, where the stream first surfaces between rough, unrounded cobble blocks. Point 2 is 5 m downstream in similar material, chosen to determine how quickly water chemistry changes away from the transition zone. Point 3, designated "main creek", is 5 m further downstream, where the stream is wider and has developed a finer bedload. From there, the stream meanders through marshy deposits to the change in valley slope at Point 4, a bridge crossing nearly 700 m downstream. The stream then enters a steep, inaccessible canyon for ~5 km where sampling was not possible. Point 5 is at the downstream base of the canyon, flowing over bare bedrock before moving out into a poorly defined channel in a coarse alluvial fan. Point 6 samples the stream in this rocky channel 100 m upstream of its confluence with Piper Paradise Fisher (PPF) Creek. This alluvial fan and the confluence with PPF creek create the transition between the second-order tributary of the upper Little Elbow and the Little Elbow itself. Point 7 samples PPF creek 100 m upstream of the same confluence, and point 8 samples the stream 10 m downstream of the confluence. Sampling points 9–10 were taken at accessible locations along the main valley, and point 11 sampled a tiny surface flow of Nahahi Creek tributary 10 m above its confluence with the Little Elbow river.

2.2.2. Streamflow Sampling

Streamflow grab samples were collected mid-stream at 60% depth at all but the higher flow sampling points at Little Elbow and Elbow Falls (points 11 and 12; Figure 1), where they were collected approximately 30 cm from the stream bank for field safety concerns. One-litre polyethylene bottles were rinsed three times with streamflow then filled and capped underwater. The bottles were sealed with electrical tape around the caps and kept in a cooler for transportation. The following day the samples were vacuum filtered using 0.7 µm glass-fibre filters and then acidified with 3M HCl to pH < 2. Samples for sulphate and silica analysis were collected and field-filtered in 60 mL syringes with 0.45 µm syringe filters (Pall Laboratory, Washington, NY, USA) into 20 mL polyethylene vials. Headspace was eliminated by filling to positive meniscus before placing lids, which were sealed with electrical tape until analysis.

The longitudinal streamflow samples were collated with the analytical results for tributary and summer samples collected in July 2017 and previously reported in Campbell et al. [16]. In this previous sampling program, every 10th set of samples was taken in triplicate to ensure analytical consistency, and the same quality assurance and consistency is assumed to apply to the samples in the current study, since these data were collected mid-way through that sampling program.

At points 4, 6, and 8, water levels were high enough and field conditions safe enough to measure the streamflow rate. The rate was calculated by measuring stream area and

average velocity (discharge (m^3/s) = average area (m^2) × average velocity (m/s)). For a stream section perpendicular to flow, the entire stream width was divided along a line into 10 equal sections/segments. At each segment, instantaneous discharge and stream depth were measured using a Son Tec® Flowtracker current-velocity metre and depth gauge. For each rectangular section, discharge was calculated, and streamflow was calculated as the average of all 10 sections. Discharge at point 13 (Elbow Falls) was taken from the gauging station at Bragg Creek at Elbow Falls based on linear interpolation between historical records at Elbow Falls and that station, $r^2 = 0.92$ [45]. Discharge values for the remaining stations were then interpolated using a polynomial fit ($y = 0.0043x^2 - 0.0001x - 0.0001$, $r^2 = 1$).

2.2.3. Laboratory Analysis

Major ion concentration for all samples was analyzed with a Metrohm 930 Compact Ion Chromatography Flex system (measurement uncertainty less than ±5% (Chao 2011)), and dissolved silica and bicarbonate with a ThermoFischer Gallery (analytical error of ±0.3 mg/L). Charge balances for each sample were <±2.5%. Isotope concentrations of $\delta^{34}S$ and $\delta^{18}O$ in SO_4 were analyzed after sulfate precipitation as $BaSO_4$ by addition of $BaCl_2$ (10%). Precipitate collected on 0.45 µm Millipore filters was air dried for at least 24 h, then weighed and analyzed in an a Thermo Finnigan Delta+ XL elemental analyzer (analytical error ± 0.2‰ for $\delta^{34}S$ in SO_4 and ±1‰ for $\delta^{18}O$ in SO_4). ^{34}S is reported relative to Troilite from Canyon Diablo meteorite (CDT) and $^{18}O/^{16}O$ ratios are reported relative to Vienna Standard Mean Ocean Water (VSMOW), both in standard delta notation.

2.3. Data Analysis

To analyze aquifer contributions from interflow, siliciclastic, and carbonate aquifers, silica and sulfate concentrations were entered into the three end-member model described in Campbell et al. [16]. The reader is referred to that publication for detailed methodology, and to the Hydroshare database [46] for the code. In brief, three end-member water types were defined (interflow, siliciclastic, carbonate) based on samples from across the watershed. Using discharge (Q) as the known quantity, three linear equations were developed and solved in an inverted matrix in R, using sample concentrations of Si and SO_4 as inputs.

Equation (1) Si mass balance

$$Q_{int} \times [Si]_{int} + Q_{carb} \times [Si]_{carb} + Q_{sil} \times [Si]_{sil} = Q_{stream} \times [Si]_{stream} \quad (1)$$

Equation (2) SO_4^{2-} mass balance

$$Q_{int} \times [SO_4]_{int} + Q_{carb} \times [SO_4]_{carb} + Q_{sil} \times [SO_4]_{sil} = Q_{stream} \times [SO_4]_{stream} \quad (2)$$

Equation (3) Discharge

$$Q_{int} + Q_{carb} + Q_{sil} = Q_{stream} \quad (3)$$

This process was repeated for samples in the current study, using measured and interpolated discharge values as described in Section 2.2.2.

3. Results and Discussion

Longitudinal samples collected revealed clear spatial patterns in streamflow chemistry and isotopic composition. As is typical for eastern slopes rivers [47], total dissolved solids (TDS) generally increased with flow distance (from approximately 225 to as high as 350 mg/L; Table 1). However, silica concentrations did not follow this pattern, decreasing from 6.9 to as low as 3.68 mg/L. Conversely, sulfate concentrations increased (from 14 to >100 mg/L) along with $\delta^{34}S$ (from ~−5 to ~20 ‰).

Water oxygen isotope values normally decrease with flow distance (and decreasing elevation) [48]. Like the silica concentrations, they also displayed a counterintuitive pattern

in this study, decreasing from approximately −19.4 to as low as −19.8 over more than 500 m of elevation (Table 1, Figure 3). These counterintuitive findings are interpreted in conjunction with the distribution of rock types provide insight into the relative recharge elevation and carbonate vs. siliciclastic pathways in the Little Elbow River mountain block hydrologic system.

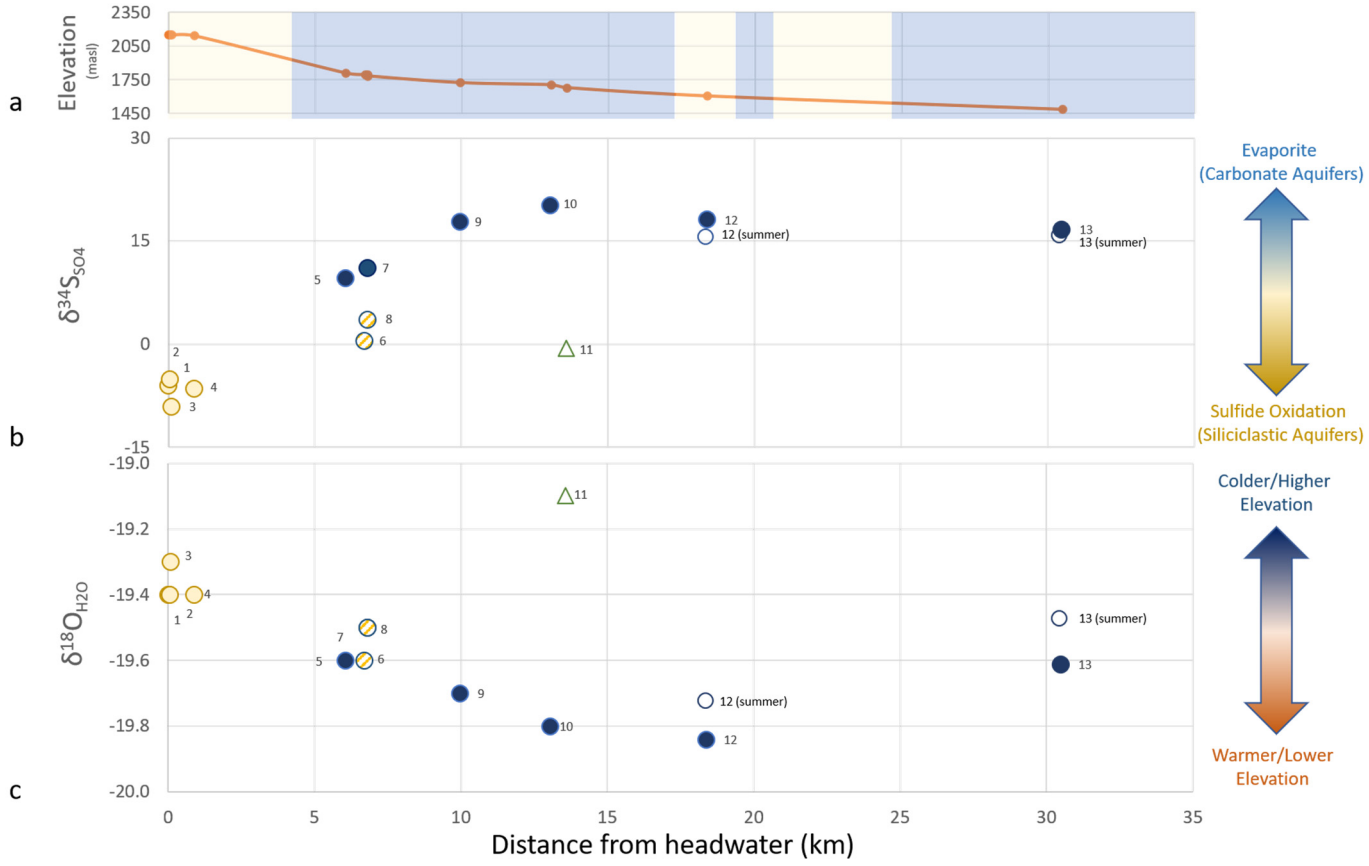

Figure 3. Longitudinal sampling results, including the (**a**) elevation profile of sampling points (orange) for Little Elbow and Elbow River, (**b**) $\delta^{34}S_{SO4}$ and (**c**) $\delta^{18}O_{H2O}$ plotted as a function of sampling distance from the headwaters (filled circles and triangle). Yellow symbols have $\delta^{34}S/\delta^{18}O_{SO4}$ values that indicate derivation of sulfate from oxidation of sulfides and blue have intermediate or evaporite derived ratios (see Figure 4). Sample point numbers (Table 1) are indicated, and the triangle symbol is for a single tributary sample. Open circles and triangle are samples from 11 July 2017 to illustrate seasonal variation occurs but does not change overall trend.

The range in sulfur isotope values is attributed to relative composition of rock–water interaction representing end-member origins of the sulfate found in the source aquifer types (Figure 4). Sulfur isotope values in sulfate were smallest in the Little Elbow Valley samples (points 1–4) falling between −4 to −10‰, samples in the transition area from the Little Elbow Valley tributary to the Little Elbow River (points 5–8) measured between 0 and 11‰, and Little Elbow River samples (9–13) measured up to 20 ‰ (Figure 4). A similar trend (from smaller values of −14‰ to as high as 6‰) were observed for oxygen isotope values in sulfate ($\delta^{18}O_{SO4}$) (Figure 4). These values indicate the primary provenance of sulfate in the streamflow shifts from siliciclastic-derived in the upper watershed to carbonate-derived along the length of the river, corresponding largely to the bedrock distribution, which is dominantly siliciclastics in the upper and carbonates in the lower watershed (Figures 1 and 3).

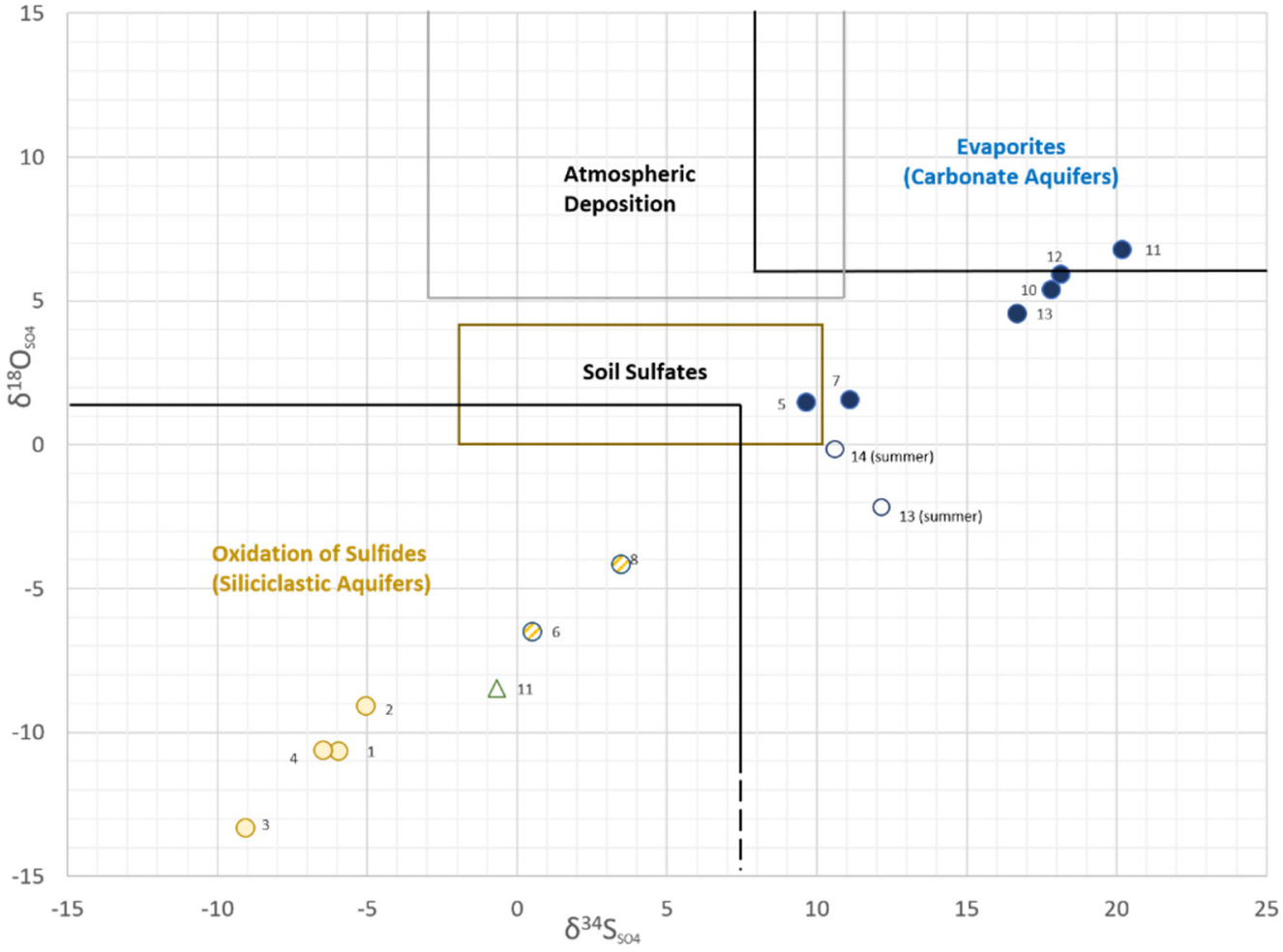

Figure 4. Cross plot of $\delta^{18}O_{SO4}$ and $\delta^{34}S_{SO4}$ for distance profile samples (filled circles and triangle). The isotopic composition of sulphate from samples collected in the open water season (July, 2017) at Elbow Falls and Little Elbow Main (open circles from Campbell et al. [16]) are included to show seasonal differences occur but do diverge from the two-end-member mixing line. The origin of SO_4 indicated by the range of isotopic values are shown by boxed areas (adapted from Krouse and Mayer, 2000). Symbol colours indicate relative contribution from rock–water interaction in two end-member aquifers (yellow—siliciclastic; blue—carbonate; hatched yellow—intermediate or mixed).

Isotopes in sulfate indicate the origin of sulfate in the water samples, but the two-end-member mixing model implied by Figure 4 does not account for water with very little water-rock interaction. This third end-member was first identified as "overland flow" by Drake and Ford [49], but Grasby et al. [50] demonstrated that overland flow is not a significant component of water in eastern slopes rivers. An end-member assigned the silica and sulfate concentrations of precipitation in the region (i.e., SiO_2 < 2 mg/L, SO_4 < 8 mg/L) was termed "interflow" by Campbell et al. [16] and incorporated into a three end-member model that encompasses the measured samples in the Little Elbow Watershed (Figure 5). In addition to interflow, the high silica (low sulfate) end-member reflects rock–water interaction in siliciclastic aquifers, while low silica (high sulfate) water is characteristic of carbonate aquifers. The model establishes the relative contribution from the two aquifer types and interflow from these silica and sulfate concentrations and can be used to better understand the interplay of water storage and streamflow within the system.

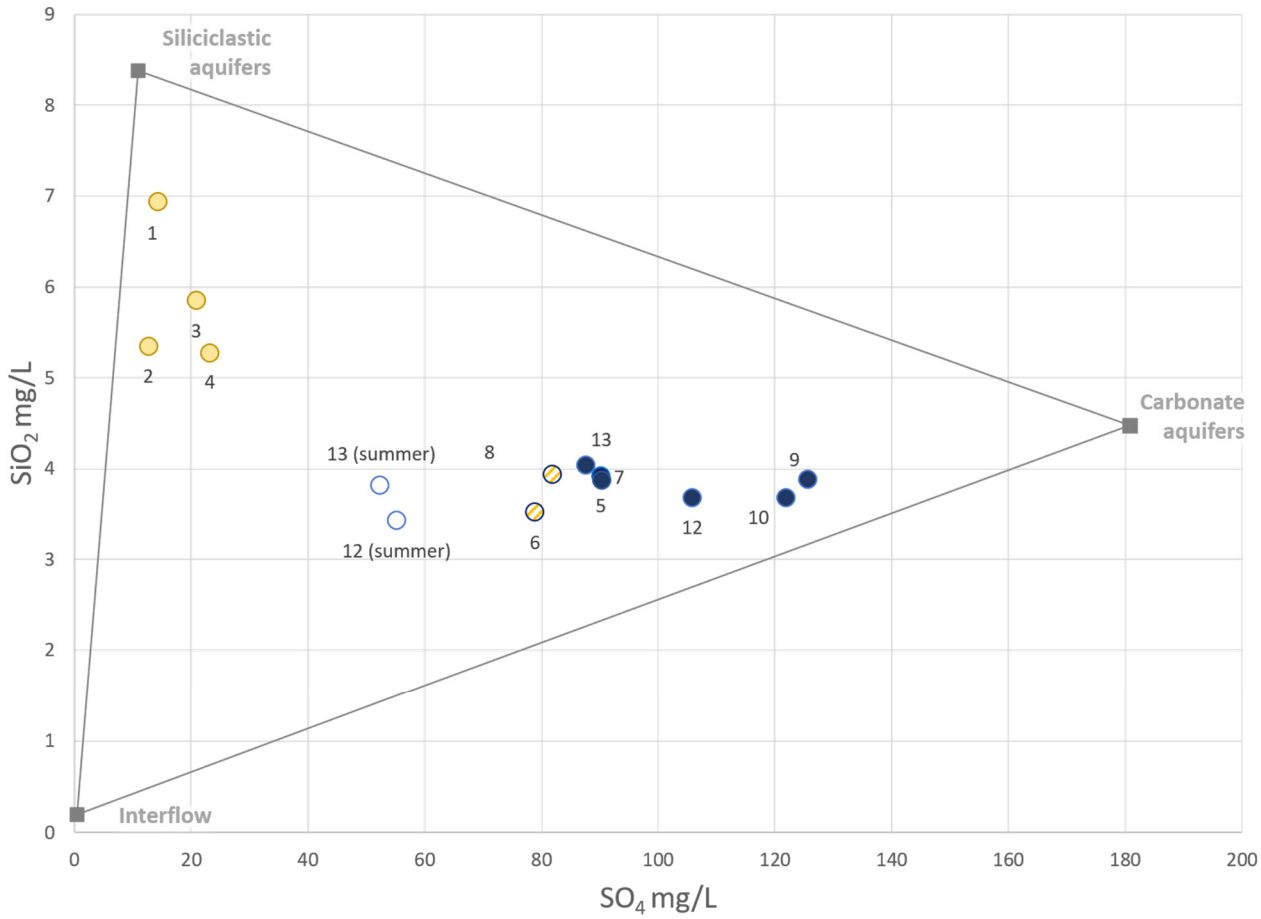

Figure 5. Silica–sulfate concentration cross plot illustrating the position of the samples collected in the current study within the three end-member mixing model previously developed for the Upper Elbow Watershed (from Campbell et al. [16]). Little Elbow Valley samples (yellow circles, points 1–4) plot toward the upper part of the siliciclastic-interflow mixing line. Samples from the transition area (hatched yellow circles, points 6 and 8) plot centrally but slightly toward carbonate end-member, and main Little Elbow River samples (blue circles, points 5, 7, 9–13) plot toward the carbonate aquifer source. Open blue circles are previously published data at points 13 and 14 from Campbell et al. [16].

Silica and sulfate concentrations in the longitudinal streamflow samples varied inversely to each other, with higher silica and low sulfate in the highest-elevation samples collected (points 1–4; sampling elevations ranging from 2142 to 2152 m asl; Table 1, Figures 3 and 5) compared to lower silica and high sulfate in the transition area and main valley (points 5–13; 1809 to 1405 m asl; Table 1, Figures 3 and 5). The samples collected in the highest part of the Little Elbow watershed (points 1–4) plot near the upper end of the siliciclastic-interflow mixing line, indicating a predominance of water (i.e., 60–90%; Table 1, Figure 5) from siliciclastic aquifers with the remainder supplied by interflow. The streamflow samples collected at in the transition area and the first Little Elbow River point (6 and 8) plot centrally but slightly toward the carbonate end member, reflecting mixing of siliciclastic-sourced water (~20%) from the Little Elbow valley with ~50% carbonate-sourced water. The remaining main valley points (9–12) plot toward the carbonate end-member (i.e., >65% carbonate end member and <10% siliciclastic), signifying dominantly carbonate aquifer contributions. The Elbow Falls sample (point 13) plots more centrally, reflecting increased siliciclastic contributions as the river flows through longer stretches of siliciclastic bedrock before reaching the falls (Figures 1–3).

The silica and sulfate concentrations and sulfate isotopes provide multiple lines of evidence to support interpretations of siliciclastic and carbonate aquifer contributions varying spatially in the Little Elbow mountain block. On their own, however, they do not

paint a clear picture of how the water moves through the hydrologic system. The water isotopes in streamflow (i.e., $\delta^{18}O_{H2O}$ and $\delta^{2}H_{H2O}$) provide further insight in this regard.

In general, river water isotopes tend to increase as elevation decreases [49], following global patterns of water isotopes in precipitation [43,44]. Colder and higher-elevation precipitation tends to enter rivers at higher elevations while warmer and lower-elevation precipitation enters rivers at lower elevation. The $\delta^{18}O/\delta^{2}H$ in precipitation for the Little Elbow system (Figure 6) highlights this pattern: average monthly water isotope values in precipitation for winter (November–March, Figure 5 blue squares) and summer (April–September, orange squares) are distinct and emphasize the difference in precipitation temperatures between the seasons. Water isotope values in Little Elbow streamflow are dampened due to mixing in groundwater storage and transport [13,51], but separation between the siliciclastic-stored and carbonate-stored water is evident, with overlap for the intermediate or mixed-source samples (Figure 6, inset).

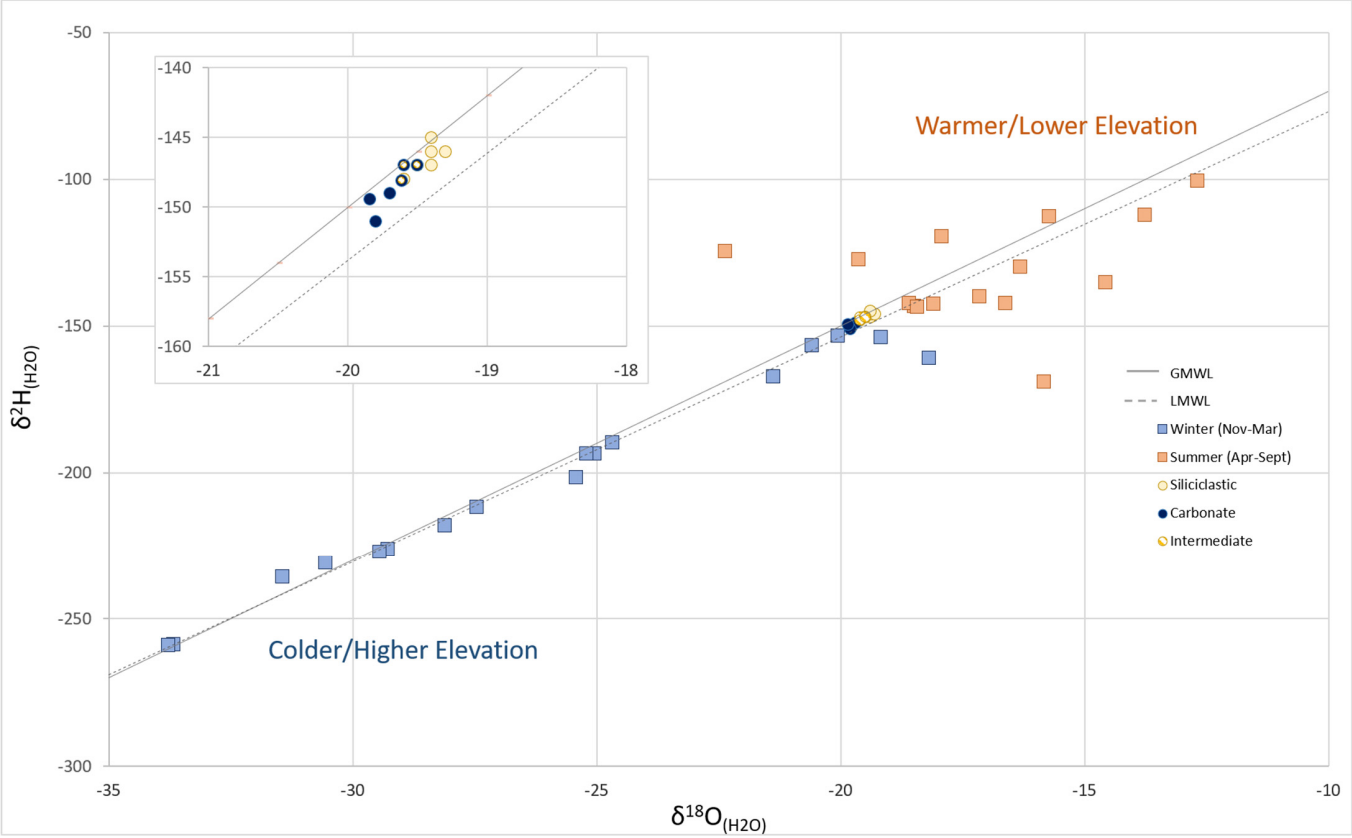

Figure 6. Cross plot of $\delta^{18}O$ and $\delta^{2}H$ in precipitation (filled squares; from Campbell et al. [16]) and longitudinal streamflow samples (circles). The global meteoric water line (solid grey) and local meteoric water line (dashed grey, from Peng et al., 2004 [52]) are shown. Colder and/or higher-elevation precipitation has lower $\delta^{18}O$ and $\delta^{2}H$ values (blue squares) and warmer and/or lower-elevation precipitation has higher values (orange squares). Siliciclastic-stored streamflow (yellow circles) falls in the warmer/lower-elevation region and carbonate-stored streamflow (blue circles) in the colder/higher-elevation region. Inset shows details of streamflow samples.

However, these global patterns do not necessarily hold at smaller scales, and the deviations can provide valuable information. In the Little Elbow longitudinal streamflow samples, the water oxygen isotope values ($\delta^{18}O_{H2O}$) in samples counterintuitively decreased with decreasing streamflow sampling elevation (Figure 4), indicating that streamflow in the lower-elevation main valley is derived from colder or higher-elevation precipitation than that in its valley nearer the headwaters. These data introduce some nuance to the concepts that water infiltrating bedrock tends to stay within the upper 20 m with only

20% entering deeper flow systems [11,12], and that there is a functional distinction between recharge processes in local, intermediate, and regional pathways, or indeed between mountain aquifer recharge and MBR [6]. There is ~450 m elevation difference between the upper Little Elbow valley sampling points and those in the main valley (i.e., between sampling points 1 and 8; Table 1), and typically >1000 m between the Elbow River and the adjacent carbonate mountain peaks. The streamflow sample at Point 12 highlights this point: although the sampling point is at 1605 m elevation, approximately 500 m lower than adjacent peaks, the $\delta^{18}O$ of 19.8‰ indicates that the water is dominated by cold or high-elevation precipitation.

Water isotopes, silica concentrations, and sulfate concentrations in the longitudinal samples suggest that the colder, higher-elevation precipitation travels through intermediate and deep flow systems, falling as snow on the cliff-forming carbonate rocks and infiltrating as melt through their well-developed fracture systems down to the bedrock of the main valley before becoming streamflow. In contrast, more of the warmer, lower-elevation precipitation infiltrates in the siliciclastic valleys and surfaces as streamflow through local flow systems (Figures 1 and 4). The Graphical Abstract illustrates this process, with the warmer, lower-elevation precipitation infiltrating into the local flow systems in the upper valley, producing siliciclastic aquifer-hosted streamflow with low $\delta^{18}O$ of approximately 19.2‰, and, colder, higher-elevation precipitation infiltrating into intermediate and regional flow systems, producing dominantly carbonate aquifer-hosted streamflow.

Details around infiltration in the carbonate units could fall within the current paradigm; for example, the majority of infiltration could remain in the upper 20 m of the mountainside, with more oblique travel down the mountain than vertical. Future work using drilled groundwater wells in combination with hydrologic modelling, similar to Manning et al. [11], could help delineate these details. Nevertheless, it is clear that in the Little Elbow hydrologic system, the boundaries between mountain aquifer recharge and mountain block recharge are blurry. For investigating lowland recharge these distinctions can be useful, but when considering mountain block hydrology more generally, and the relationships between recharge and streamflow within the mountain block, they may introduce artificial divides because the same recharge processes that produce streams in the mountains must logically also produce deep mountain groundwater.

A final consideration highlighted by these longitudinal streamflow data is the effect of climate change on the Little Elbow hydrologic system. In this area, as elsewhere, warming temperatures are producing earlier snowmelt [36]. The late-season sampling date (October 26) for the longitudinal survey was chosen to sample streamflow as characteristic of winter baseflow as possible, to assess the relative contributions of aquifers in the hydrologic system. Low silica, high sulfate concentrations with high $\delta^{34}S_{SO4}$ and $\delta^{18}O_{SO4}$ in the main valley samples (points 9,10,12,13) indicate that the majority of overwinter baseflow in the Elbow River is supplied by carbonate aquifers (Figure 5). The relatively low value of $\delta^{18}O_{H2O}$ indicates this water originates as cold/high-elevation winter precipitation (Figure 6). This interpretation is supported by the July samples for Little Elbow and Elbow Falls sampling locations—both plot much further toward the interflow-siliciclastic mixing line than the late October samples, emphasizing the higher seasonal contribution from interflow and siliciclastic aquifers in summer (Figure 3). Thus, winter baseflow is dependent on previous winters′ precipitation, and changes in the volume and timing of snowfall and snowmelt may impact future winter baseflow.

4. Conclusions

In the Elbow River catchment, nested mountain aquifer flow systems convey lower-elevation, warmer precipitation to headwater streams in siliciclastic-bedrock valleys, while high-elevation, colder precipitation to lower-elevation river reaches via snowmelt infiltration into cliff-forming carbonate bedrock. The large elevation difference between infiltration areas and main valley streamflow suggests less separation between intermediate and deep flow pathways, or mountain aquifer and mountain block recharge, than previously thought.

Longitudinal streamflow sampling at the end of the open water season indicates that winter baseflow is generated mainly from carbonate aquifers and mainly from high-elevation winter precipitation. This dependence means winter streamflow in the Elbow River is vulnerable to changes in winter precipitation volume and timing.

Author Contributions: Conceptualization, É.M.S.C. and M.C.R.; methodology, É.M.S.C.; formal analysis, É.M.S.C.; resources, M.C.R.; data curation, É.M.S.C.; writing—original draft preparation, É.M.S.C.; writing—review and editing, É.M.S.C. and M.C.R.; visualization, É.M.S.C.; supervision, M.C.R.; project administration, É.M.S.C.; funding acquisition, É.M.S.C. and M.C.R. All authors have read and agreed to the published version of the manuscript.

Funding: Funding for this research was provided by the Bow River Basin Council.

Institutional Review Board Statement: Not applicable.

Informed Consent Statement: Not applicable.

Data Availability Statement: Data are available from the Hydroshare database, available online: http://www.hydroshare.org/resource/71ae1df804b6474baee58c1fe93953d0 (accessed on 12 August 2021).

Acknowledgments: Tom Currie created the Graphical Abstract based on technical discussions with É.C. Heather Reader volunteered as field partner for longitudinal sampling. Kananaskis Provincial Park Ranger Rod Gow and Alberta Parks' Melanie Percy provided restricted road access. Farzin Malekani and Steve Taylor supervised student research assistants Megan Leung and Sofija Stanic for lab analyses.

Conflicts of Interest: The authors declare no conflict of interest. The funders had no role in the design of the study; in the collection, analyses, or interpretation of data; in the writing of the manuscript, or in the decision to publish the results.

References

1. Viviroli, D.; Kummu, M.; Meybeck, M.; Kallio, M.; Wada, Y. Increasing dependence of lowland populations on mountain water resources. *Nat. Sustain.* **2020**, *3*, 917–928. [CrossRef]
2. Somers, L.D.; McKenzie, J.M. A review of groundwater in high mountain environments. *Wiley Interdiscip. Rev. Water* **2020**, *7*, 1–27. [CrossRef]
3. Pepin, N.; Bradley, R.S.; Diaz, H.F.; Baraer, M.; Caceres, E.B.; Forsythe, N.; Fowler, H.; Greenwood, G.; Hashmi, M.Z.; Liu, X.D.; et al. Elevation-dependent warming in mountain regions of the world. *Nat. Clim. Chang.* **2015**, *5*, 424–430.
4. Musselman, K.N.; Addor, N.; Vano, J.A.; Molotch, N.P. Winter melt trends portend widespread declines in snow water resources. *Nat. Clim. Chang.* **2021**, *11*, 418–424. [CrossRef] [PubMed]
5. Wilson, J.L.; Guan, H.; Phillips, F.M.; Hogan, J.; Scanlon, B.; Agu, W. Mountain-Block Hydrology and Mountain-Front Recharge. *Groundw. Recharg. Desert Environ. Southwest US* **2004**, *9*, 113–137.
6. Markovich, K.H.; Manning, A.H.; Condon, L.E.; McIntosh, J.C. Mountain-Block Recharge: A Review of Current Understanding. *Water Resour. Res.* **2019**, *55*, 8278–8304. [CrossRef]
7. Hayashi, M. Alpine Hydrogeology: The Critical Role of Groundwater in Sourcing the Headwaters of the World. *Groundwater* **2020**, *58*, 498–510. [CrossRef] [PubMed]
8. Christensen, C.W.; Hayashi, M.; Bentley, L.R. Hydrogeological characterization of an alpine aquifer system in the Canadian Rocky Mountains. *Hydrogeol. J.* **2020**, *28*, 1871–1890. [CrossRef]
9. Käser, D.; Hunkeler, D. Contribution of alluvial groundwater to the outflow of mountainous catchments. *Water Resour. Res.* **2016**, *52*, 680–697. [CrossRef]
10. Tóth, J. A theoretical analysis of groundwater flow in small drainage basins. *J. Geophys. Res.* **1963**, *68*, 4795–4812. [CrossRef]
11. Manning, A.H.; Ball, L.B.; Wanty, R.B.; Williams, K.H. Direct Observation of the Depth of Active Groundwater Circulation in an Alpine Watershed. *Water Resour. Res.* **2021**, *57*. [CrossRef]
12. Smerdon, B.D.; Allen, D.M.; Grasby, S.E.; Berg, M.A. An approach for predicting groundwater recharge in mountainous watersheds. *J. Hydrol.* **2009**, *365*, 156–172. [CrossRef]
13. Campbell, É.M.S.; Pavlovskii, I.; Ryan, M.C. Snowpack disrupts relationship between young water fraction and isotope amplitude ratio; approximately one fifth of mountain streamflow less than one year old. *Hydrol. Process.* **2020**, *34*, 4762–4775. [CrossRef]
14. Winter, T.C. The role of ground water in generating streamflow in headwater areas and in maintaining base flow. *J. Am. Water Resour. Assoc.* **2007**, *43*, 15–25. [CrossRef]
15. Paznekas, A.; Hayashi, M. Groundwater contribution to winter streamflow in the Canadian Rockies. *Can. Water Resour. J.* **2016**, *41*, 484–499. [CrossRef]

16. Campbell, É.M.S.; Lagasca, P.A.; Stanic, S.; Zhang, Y.; Ryan, M.C. Insight into watershed hydrodynamics using silica, sulfate, and tritium: Source aquifers and water age in a mountain river. *Appl. Geochem.* **2021**, 105070. [CrossRef]
17. Klaus, J.; McDonnell, J.J. Hydrograph separation using stable isotopes: Review and evaluation. *J. Hydrol.* **2013**, *505*, 47–64. [CrossRef]
18. McGuire, K.; McDonnell, J.J. A review and evaluation of catchment transit time modeling. *J. Hydrol.* **2006**, *330*, 543–563. [CrossRef]
19. Feng, X.; Faiia, A.M.; Posmentier, E.S. Seasonality of isotopes in precipitation: A global perspective. *J. Geophys. Res. Atmos.* **2009**, *114*, 1–13. [CrossRef]
20. Beria, H.; Larsen, J.R.; Ceperley, N.C.; Michelon, A.; Vennemann, T.; Schaefli, B. Understanding snow hydrological processes through the lens of stable water isotopes. *WIREs Water* **2018**, *5*, e1311. [CrossRef]
21. Jasechko, S.; Wassenaar, L.I.; Mayer, B. Isotopic evidence for widespread cold-season-biased groundwater recharge and young streamflow across central Canada. *Hydrol. Process.* **2017**, *31*, 2196–2209. [CrossRef]
22. Hoeg, S.; Uhlenbrook, S.; Leibundgut, C. Hydrograph separation in a mountainous catchment—Combining hydrochemical and isotopic tracers. *Hydrol. Process.* **2000**, *14*, 1199–1216. [CrossRef]
23. Benettin, P.; Bailey, S.W.; Campbell, J.L.; Green, M.B.; Rinaldo, A.; Likens, G.E.; McGuire, K.J.; Botter, G. Linking water age and solute dynamics in streamflow at the Hubbard Brook Experimental Forest, NH, USA. *Water Resour. Res.* **2015**, *51*, 9256–9272. [CrossRef]
24. Peters, N.E.; Burns, D.A.; Aulenbach, B.T. Evaluation of High-Frequency Mean Streamwater Transit-Time Estimates Using Groundwater Age and Dissolved Silica Concentrations in a Small Forested Watershed. *Aquat. Geochem.* **2014**, *20*, 183–202. [CrossRef]
25. Haines, T.S.; Lloyd, J.W. Controls on silica in groundwater environments in the United Kingdom. *J. Hydrol.* **1985**, *81*, 277–295. [CrossRef]
26. Clow, D.W.; Mast, M.A. Mechanisms for chemostatic behavior in catchments: Implications for CO_2 consumption by mineral weathering. *Chem. Geol.* **2010**, *269*, 40–51. [CrossRef]
27. Maher, K.; Chamberlain, C.P. Hydrologic Regulation of Chemical. *Science* **2014**, *343*, 1502–1504. [CrossRef] [PubMed]
28. Donato, M.M. *Surface-Water/Ground-Water Relations in the Lemhi River Basin, East-Central Idaho*; US Geological Survey: Reston, VA, USA, 1998.
29. Manwell, B.R.; Ryan, M.C. Chloride as an Indicator of Non-point Source Contaminant Migration in a Sha: EBSCOhost. *Water Qual. Res. J.* **2006**, *41*, 383–397. [CrossRef]
30. Valeo, C.; Xiang, Z.; Bouchart, F.J.; Yeung, P.; Ryan, M.C. Climate change impacts in the Elbow River watershed. *Can. Water Resour. J.* **2007**, *32*, 285–302. [CrossRef]
31. Alberta Environment and Sustainable Resource Development. Alberta River Basins. 2019. Available online: Rivers.alberta.ca (accessed on 15 July 2021).
32. Wijesekara, G.N.; Farjad, B.; Gupta, A.; Qiao, Y.; Delaney, P.; Marceau, D.J. A Comprehensive Land-Use/Hydrological Modeling System for Scenario Simulations in the Elbow River Watershed. *Environ. Manag.* **2014**, *53*, 357–381. [CrossRef] [PubMed]
33. EPCOR Water Services Inc. *Source Water Protection Plan*; EPCOR Water Services Inc.: Edmonton, AB, Canada, 2018.
34. Jacques, J.M.S.; Lapp, S.L.; Zhao, Y.; Barrow, E.M.; Sauchyn, D.J. Twenty-first century central Rocky Mountain river discharge scenarios undergreenhouse forcing. *Quat. Int.* **2013**, *310*, 34–46. [CrossRef]
35. Farjad, B.; Gupta, A.; Marceau, D.J. Annual and Seasonal Variations of Hydrological Processes Under Climate Change Scenarios in Two Sub-Catchments of a Complex Watershed. *Water Resour. Manag.* **2016**, *30*, 2851–2865. [CrossRef]
36. Chernos, M.; MacDonald, R.J.; Nemeth, M.W.; Craig, J.R. Current and future projections of glacier contribution to streamflow in the upper Athabasca River Basin. *Can. Water Resour. J.* **2020**, *45*, 324–344. [CrossRef]
37. Environment Canada. *Historical Climate Data*; Environment Canada, 2019. Available online: https://climate.weather.gc.ca/ (accessed on 13 August 2021).
38. Alberta, J.A.; Prior, E.R.; Hathway, G.J.; Glombick, B.; Pana, P.M.; Banks, D.I.; Hay, C.J.; Schneider, D.C.; Grobe, C.L.; Elgr, M.; et al. Bedrock Geology of Alberta, AER/AGS Map 601, scale 1:1,000,000. *Acco. AGS Open File Rep.* **2013**, *2*, 2.
39. Alberta Environment and Sustainable Resource Development. Natural Regions and Subregions of Alberta (Shapefile). 2005. Available online: https://www.albertaparks.ca/media/429607/natural_regions_subregions_of_alberta.zip (accessed on 15 July 2021).
40. CA-AB-EPS-02-0001, Map of Alberta. *Free Vector Maps*. 2021. Available online: https://freevectormaps.com/canada/alberta/CA-AB-EPS-02-0001?ref=atr (accessed on 6 August 2021).
41. Evers, H.J.; Thorpe, J.E. *Structural Geology of the Foothills between Savanna Creek and Panther River*; Canadian Society of Petroleum Geologists: Calgary, AB, Canada, 1975.
42. Krouse, H.R.; Mayer, B. Sulphur and Oxygen Isotopes in Sulphate. In *Environmental Tracers in Subsurface Hydrology*; Cook, P.G., Herczeg, A.L., Eds.; Springer: Boston, MA, USA, 2000; pp. 195–231.
43. Gat, J.R. Oxygen and Hydrogen Isotopes in the Hydrologic Cycle. *Annu. Rev. Earth Planet. Sci.* **1996**, *24*, 225–262. [CrossRef]
44. Rozanski, K.; Araguás-Araguás, L.; Gonfiantini, R. Isotopic Patterns in Modern Global Precipitation. *Wash. Am. Geophys. Union* **1993**, *78*, 1.
45. Campbell, E.; Pavlovskii, I.; Ryan, M.C. Overwinter Snowpack and Young Water Fraction Modelling (Elbow River Data). *Hydroshare* **2019**. Available online: http://www.hydroshare.org/resource/889a805e3b8a4073bf8312839914cde4%0A (accessed on 12 August 2021).

46. Campbell, É.M.S. Upper Elbow River Watershed Silica, Sulfate, Tritium | CUAHSI HydroShare. *Hydroshare* **2021**. Available online: https://www.hydroshare.org/resource/71ae1df804b6474baee58c1fe93953d0/ (accessed on 5 August 2021).
47. Grasby, S.E.; Hutcheon, I. Chemical dynamics and weathering rates of a carbonate basin Bow River, southern Alberta. *Appl. Geochem.* **2000**, *15*, 67–77. [CrossRef]
48. Gibson, J.J.; Fekete, B.M.; Bowen, G.J. Stable isotopes in large scale hydrological applications. In *Isoscapes: Understanding Movement, Pattern, and Process on Earth through Isotope Mapping*; Springer: Dordrecht, The Netherlands, 2010; pp. 389–405.
49. Drake, J.J.; Ford, D.C. Hydrochemistry of the Athabasca and North Saskatchewan Rivers in the Rocky Mountains of Canada. *Water Resour. Res.* **1974**, *10*, 1192–1198. [CrossRef]
50. Grasby, S.E.; Hutcheon, I.; McFarland, L. Surface-water-groundwater interaction and the influence of ion exchange reactions on river chemistry. *Geology* **1999**, *27*, 223–226. [CrossRef]
51. Taylor, S.; Feng, X.; Kirchner, J.W.; Osterhuber, R.; Klaue, B.; Renshaw, C.E. Isotopic evolution of a seasonal snowpack and its melt. *Water Resour. Res.* **2001**, *37*, 759–769. [CrossRef]
52. Peng, H.; Mayer, B.; Harris, S.; Krouse, H.R. A 10-yr record of stable isotope ratios of hydrogen and oxygen. *Tellus* **2004**, *56*, 147–159. [CrossRef]